Virology 536 (2019) 68–77

Contents lists available at ScienceDirect

Virology

journal homepage: www.elsevier.com/locate/virology

Symptom recovery is affected by Cucumber mosaic virus coat protein phosphorylation

Katalin Nemes[a], Ákos Gellért[b], Károly Bóka[c], Pál Vági[c], Katalin Salánki[a,*,1]

[a] Plant Protection Institute, Centre for Agricultural Research, Hungarian Academy of Sciences, Budapest, Hungary
[b] Institute for Veterinary Medical Research, Centre for Agricultural Research, Hungarian Academy of Sciences, Budapest, Hungary
[c] Department of Plant Anatomy, Eötvös Loránd University, Faculty of Sciences, Budapest, Hungary

ARTICLE INFO

Keywords:
CP
Symptom recovery
Phosphorylation
VSR activity

ABSTRACT

Cucumber mosaic virus induces specific recovery phenotype, namely cyclic mosaic symptoms on tobacco plants. We provide further evidence that besides the 2b suppressor protein, the coat protein (CP) also has a role in symptom recovery and it is connected to its phosphorylation. We analyzed the impact of the phosphorylated (S148D) and the non-phosphorylated (S148A) state of CP148 Ser on symptom formation, virion stability and the effect of CP and its mutants on 2b-mediated local GFP-silencing. We demonstrated that a single aa change could be responsible for preventing the recovery phenomenon as replacing the phosphorylatable Ser with Ala in the 148aa position abolishing the cyclic phenomenon. CP/S148A mutation equilibrates the accumulation of the virus during the infection both at RNA and protein level in *N. tabacum* L. cv Xanthi plants. In summary, we determined a regulatory effect of the CMV CP on the self-attenuation mechanism and downregulation of the suppressor effect of the 2b protein.

1. Introduction

Cucumber mosaic virus (CMV) is one of the most important plant virus both as a devastating agent in agriculture and as an object of thousands of studies (Scholthof et al., 2011). In addition, it has an extremely wide host range (Edwardson and Christie, 1991). CMV has only five proteins encoded by its three genomic RNAs. These proteins have to accomplish the complete replication cycle of the virus, the cell-to-cell and long distance movement besides symptom formation of the virus in tight interaction with the host proteins which can be different in distinct hosts. Therefore, beyond the primary function of a viral protein, several additional roles could be addressed to it. The 1a and 2a proteins are components of the RNA replication complex, the 2b protein functions as the gene silencing suppressor, while the 3a protein is the movement protein (Palukaitis and García-Arenal, 2003). The primary function of the CMV coat proteins (CPs) is the genome encapsidation, however, due to the limited number of viral proteins, it has a role in the movement of the virus (both in cell-to-cell and systemic movement) (Kaplan et al., 1997; Wong et al., 1999), aphid transmission (Chen and Francki, 1990), host range determination (Ryu et al., 1998) and symptom induction on different plant species as well (Suzuki et al., 1995; Qiu et al., 2018).

Posttranslational modifications allow the proteins to modify their structure and function. In the case of CMV, the phosphorylation of the 1a and 2b proteins in infected plants were verified (Kim et al., 2002; Nemes et al., 2017). Serine phosphorylation of the movement protein (MP) in transgenic plants was also detected (Matsushita et al., 2002), but it was not analyzed in the course of virus infection. The 2a protein phosphorylation located in the N-terminal 126 amino acid region inhibits formation of the replicase complex (Kim et al., 2002). The 2b protein phosphorylation was predicted to the 40/42 Ser position (Lucy et al., 2000). Recently, 2b phosphorylation and its role in regulation of subcellular localization were demonstrated directly. Namely, the phosphorylated 2b protein accumulates only in the cytoplasm and it is unable enter the nucleus, and it also controls the suppressor activity of the 2b protein (Nemes et al., 2017).

The effect of CP phosphorylation in the life cycle of plant viruses is multifarious. Its role was demonstrated in translational activation in the case of potato virus X (Atabekov et al., 2001), in virus infectivity and symptom development in the case of cauliflower mosaic virus (Chapdelaine et al., 2002) or timing of viral infection in the case of brome mosaic virus (Hoover et al., 2016). Phosphorylation of bamboo mosaic virus CP regulates the cell-to-cell movement by modulation of RNA binding affinity (Hung et al., 2014). RNA-binding is also inhibited

* Corresponding author.
E-mail address: salanki.katalin@agrar.mta.hu (K. Salánki).
[1] Herman Ottó Road 15, Budapest, H-1022, Hungary.

https://doi.org/10.1016/j.virol.2019.08.003
Received 27 April 2019; Received in revised form 1 August 2019; Accepted 3 August 2019
Available online 04 August 2019

Table 1
List of primers used for mutagenesis creating CP/S148A, CP/S148D and CP/S148sil mutants. The mutated nucleotide positions are highlighted.

Primer name	Primer sequence (5′- 3′)	Encoded aa
Rs-CMV_rev	GGACTAGTACCGGTCAGGCTCCGTCCGCG	S
CP/148sil_rev	GGACTAGTACCGGAGTGGCTCCGTCCGCG	S
CP/S148A_rev	GGACTAGTACCGGTGCGGCTCCGTCCGCG	A
CP/S148D_rev	GGACTAGTACCGGATCGGCTCCGTCCGCG	D
CP_148mut_for	CGACTAGTTTATCAGTATGCCGCA	

in the case of phosphorylation of potato virus A CP by CK2, prevention of CP phosphorylation disrupts cell-to-cell and long distance movement (Ivanov et al., 2001, 2003). CP phosphorylation of potato virus A has role in translation-replication switching (Lõhmus et al., 2017). CP phosphorylation of beet black scorch virus plays essential role in long distance movement of the virus that involves the assembly and stability of the virus particle (Zhao et al., 2015).

In our present work, the phosphorylation of CMV CP is demonstrated. We analyzed the effects of mimicked phosphorylated (S148D) and non-phosphorylated (S148A) states of CMV CP on symptom formation, virion stability, and on the 2b-mediated local GFP-silencing.

2. Materials and methods

2.1. Virus inoculation

The Rs strain of CMV and the infectious transcripts (pRs1, pRs2, pRs3) have been described previously (Diveki et al., 2004). The Ser (S) amino acid at residue 148 of the CP was replaced to Ala (A) and to Asp (D) with PCR based mutagenesis using the primers detailed in Table 1. A further mutant, labeled as CP/S148sil was also created in which the coding region was mutated but the Ser 148 was unaltered. The resulted mutants were designated as CP/S148A, CP/S148D and CP/S148sil, respectively.

Nicotiana tabacum L. cv Xanthi plants at three-leaf-stage were mechanically inoculated with the RNA3 *in vitro* transcripts of Rs-CMV or mutants supplemented with RNA 1, RNA 2 transcripts. All the other test plants were inoculated with purified virions. The plants were grown in a temperature-controlled growth chamber with conditions of 16 h of light at 24 °C and 8 h of dark at 21 °C. Symptom development was observed during the following 2 months period. The different leaf stages were numbered from the top to the bottom (L1-14, L1 is the youngest leaf while L14 signifies the oldest leaves).

2.2. Western blot analyses

Protein extracts from *N. tabacum* L. cv Xanthi, *N. benthamiana,*

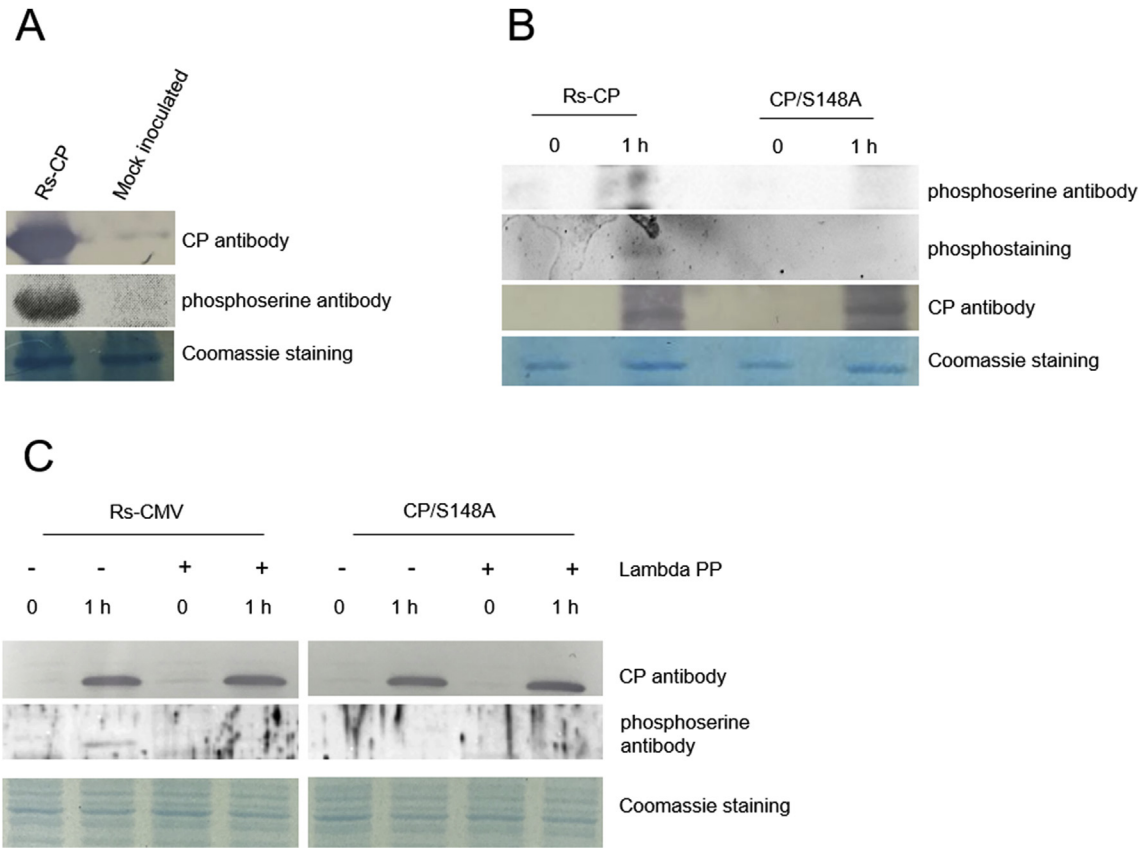

Fig. 1. CMV CP is phosphorylated in infected tobacco plants. (A) *In vivo* phosphorylation of CMV CP in infected *N. tabacum* L. cv Xanthi plant. CP and phosphoserine antibodies were used to detect phosphorylation of CP in infected *N. tabacum* L. cv Xanthi test plants. Coomassie staining was used to monitor the equivalence of protein loading. (B) Western blot analysis of phosphorylation of *Escherichia coli* expressed Rs-CP and CP/S148A. The samples were separated by SDS-PAGE, transferred to membrane and probed with phosphoserine antibody. Protein gel was also stained with phos-tag phosphoprotein stain. The difference between the phospho-specific stained proteins of Rs-CP and S148A and the contrast between the phosphoserine antibody detection indicates that position 148 is phosphorylated. The presence of expressed CPs were verified with CP antibody. Coomassie staining was used to monitor the equivalence of protein loading. (C) Lambda PP treatment of the expressed proteins. The bacterially expressed proteins were treated with Lambda Protein Phosphatase (Lambda PP) or were incubated with buffer (served as negative control). The samples were detected with phosphoserine and CP antibodies. The difference between the non-treated and treated Rs-CP indicate that Rs-CP is phosphorylated.

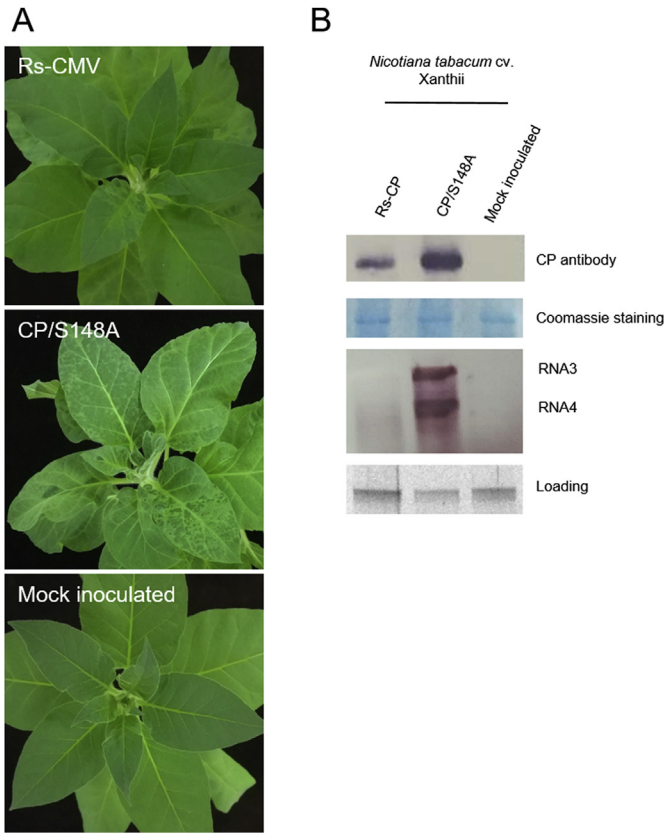

Fig. 2. The effect of CP S148 on symptoms, CP and RNA accumulation on *Nicotiana tabacum* L. cv Xanthi plants. (A) Symptoms induced by Rs-CMV and CP/148A mutant on *N. tabacum* L. cv Xanthi plants. (B) Western and northern blot analyses of *N. tabacum* L. cv Xanthi plants two weeks after inoculation. The accumulation of CP in the systemic leaves was assessed with anti-CP monoclonal antibody. Coomassie stained protein from the same volume of each sample is shown below. Total RNAs were extracted from systemic leaves. The DIG-labeled probe was specific for Rs-CMV RNA3. Ethidium bromide-stained rRNA from the same volume of each sample is shown below.

Capsicum annuum cv. Brendon and *Solanum lycopersicum* cv. Moneymaker leaf samples were prepared (20 mg, fresh weight). Leaf discs of 1 cm diameter were ground and homogenized in an ice-cold mortar in 0.2 ml of 1x protein sample buffer (4x buffer: 40% Glycerol, 240 mM Tris/HCl pH 6.8, 8% SDS, 0.04% bromophenol blue and 5% beta-mercaptoethanol) heated at 95 °C for 5 min, and centrifuged (5 min at 10,000 g) to remove insoluble material. Aliquots of the supernatant (1–10 µl) were separated on 12% SDS-PAGE gels. An equal amount of the loading was verified by Coomassie staining. After electrophoresis, proteins were transferred to Hybond-C membrane (GE Healthcare Bio-Sciences) and subjected to immunoblot analysis with CP, GFP (Invitrogen), 2b protein (Agrisera) or phosphoserine antibody (Qiagen). As secondary antibody HRP-conjugate anti-mouse IgG (Agrisrea) or AP-conjugate anti-rabbit IgG (BioRad) was used.

2.3. Protein expression and phosphatase treatment

cDNAs of wild-type (Rs-CMV) and 148A mutant CPs were introduced to pET-28 plasmids and transformed into BL21 (DE3)pLysE *Escherichia coli* (Thermo Fisher Scientific). 1 h after induction with 0.2 mM Isopropyl β-D-1-thiogalactopyranoside at 37 °C, 1 ml of bacteria solutions were centrifuged (1 min at 10,000 × *g*) and pellets were re-suspended with 1x protein sample buffer. The bacterially expressed proteins were incubated with Lambda Protein Phosphatase (Lambda PP) for 30 min on 30 °C (New England BioLabs, Ipswich, MA, USA) or were incubated with the buffer (10X NEB buffer). The samples were detected with phosphoserine (PhosphoSerine Antibody Q5, Qiagen) and CP antibodies and stained with Coomassie.

2.4. Phosphostaining

Total proteins extracted from bacteria with 1x protein sample buffer were separated in 12% SDS-PAGE gels. Phospho-Tag™ Phosphoprotein Gel Stain was used to detect phosphoproteins according to the manufacturer instruction (GeneCopoeia).

2.5. Northern analysis

Approximately 100 ng total RNA was denatured with formaldehyde and separated in formamide-containing agarose gels and blotted on to nylon membranes (Sambrook et al., 1989). Northern blot hybridization analysis was performed with random-primed Digoxigenin-dUTP-labeled DNA fragments specific for the Rs-CMV RNA 3 sequence (Sigma-Aldrich).

2.6. Agroinfiltration, GFP imaging and qRT-PCR

Agrobacterium-mediated transient expression on *N. benthamiana* leaf was conducted by pressure infiltration as described previously (Johansen and Carrington, 2001). Agrobacterium culture of GFP-expressing strain was adjusted to a final optical density at 600 nm (OD_{600}) to 0.4. Strains expressing 2b mutants and CP were adjusted to 0.2 and 0.4, respectively.

For visual detection of GFP fluorescence patches on leaves a Blak-Ray B–100SP UV lamp (UVP) was used, and images were taken with Nikon D100 digital camera mounted with yellow lens (Hama HTMC filter).

Fresh leaf tissues (30 mg) were ground in liquid N_2 and extracted with SV Total RNA Isolation System (Promega). Reverse transcription (RT) and qRT-PCR were performed as described previously (Nemes et al., 2014). Real-time PCR was carried out in BioRad CFX96 Real-Time System machine.

2.7. Transmission electron microscopy (TEM)

Ten µl of virion solution droplets were applied onto formvar-carbon coated 300-mesh copper grids (SPI, West Chester, PA, USA). The grids were negative-stained with 2% aqueous uranyl acetate for 10 min, dried and viewed via a JEOL 1011 transmission electron microscope (Jeol Ltd., Tokyo, Japan) with 80 kV accelerating voltage and at 11,000–36,000 × magnification. Virion diameter was measured by Olympus Soft Imaging Software (Olympus Soft Imaging Solution GmbH, Münster, Germany).

2.8. Virus particle purification and RNase sensitivity assay

Virus particles were purified from infected *N. tabacum* L. cv Xanthi plants at 20 dpi as described previously (Lot et al., 1972). Ten µg of virions were treated with RNase A (0.005 µg/µl) for 0, 30, 60, 90 and 120 min at room temperature followed by RNA extraction (Promega). Two µl of RNAs were separated on agarose gel and measured with AlphaView software band analysis/densitometry (ProteinSimple, CA, USA). The amount of RNAs purified at time zero were taken as 100% and further purified RNAs were compared to time zero.

2.9. Competition experiments

The fitness of the CP/S148A mutant virus compared to the wild-type Rs-CMV was evaluated in competition experiments. *N. tabacum* L. cv Xanthi plants were mechanically inoculated with 50 ng mixture of viral RNAs of Rs-CMV and CP/S148A mutant virions. In the first case, Rs-CMV and CP/S148A mutant were inoculated in mixture in the ratio of

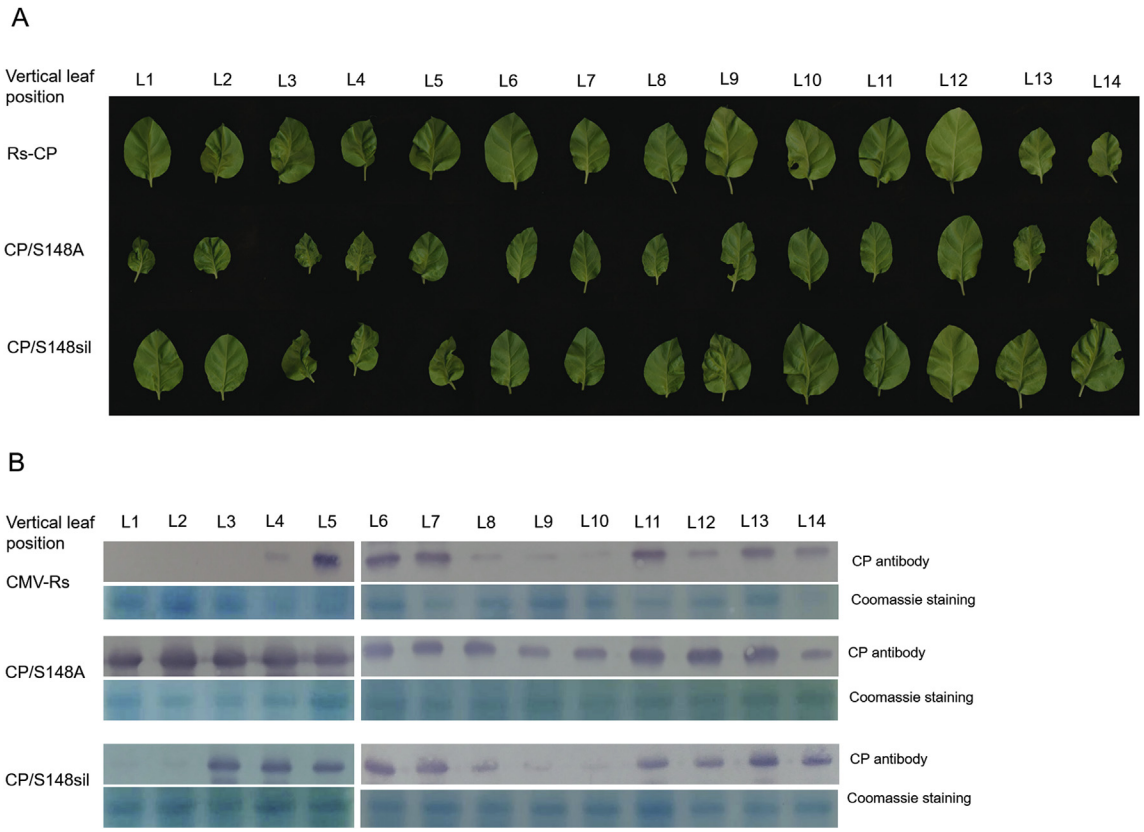

Fig. 3. Leaf stage in the course of Rs-CMV, CP/S148A and CP/148sil in 14 different stages of *Nicotiana tabucum* L. cv Xanthi plants. (A) Symptoms induced by Rs-CMV, CP/S148A and CP/148sil on *N. tabacum* L. cv Xanthi plants in different leaf stages. The consecutive leaves were numbered from the top to the bottom (L1-14, L1 is the youngest leaf while L14 signifies the oldest leaves). (B) Western blot analyses of CP accumulation in different leaf stages. CPs were detected with CP antibody and Coomassie staining was used to monitor the equivalence of protein loading.

1:1 on whole leaves of *N. tabacum* L. cv Xanthi plants. In the second case, Rs-CMV and CP/S148A mutant were inoculated in the ratio of 1:1, but separately on the opposite half leaves. Inoculation was also implemented in the ratio of 70-30% of Rs-CMV and CP/S148A and *vice versa*, both as a mixture on the whole leaves and separated on the opposite half of the leaves as well. The accumulation of the viruses was analyzed two weeks post inoculation in systemically infected leaves by nucleotide sequence determination of the RT-PCR product of the CP genes.

2.10. Molecular modeling and graphics

The original Fny-CMV X-ray structure (Smith et al., 2000) (PDB ID: 1F15) was used to generate the Rs-CMV wild and mutant models because only the 107th amino acid differs between the two strains. To create the wild Rs-CMV CP model Leu 107 was mutated to Ile in the original Fny-CMV CP structure using the academic version of the Schrödinger Maestro (Schrödinger, 2019) (https://www.schrodinger.com/freemaestro). After mutation a short local geometry optimization was performed on the altered residue atoms. The Rs-CMV CP/S148A and Rs-CMV CP/S148D mutant models were built in the same way. Electrostatic potential maps were calculated with Adaptive Poisson–-Boltzmann Solver (APBS) version 1.3 (Baker et al., 2001) using the linearized Poisson–Boltzmann method (Gilson et al., 1987) with a dielectric constant of 78.0 and 2 for the water solvent and protein core, respectively. The partial charges for the electrostatic potential calculations were calculated with PDB2PQR (Dolinsky et al., 2004). Molecular graphics were created with VMD version 1.9.3 (Humphrey et al., 1996) and with PyMOL 1.8.0.3 Molecular Graphics System (https://pymol.org/2).

3. Results

3.1. Phosphorylation of CMV CP

In order to determine whether CMV CP is phosphorylated *in vivo*, total protein was extracted from symptomatic leaves of *Nicotiana tabacum* L. cv Xanthi plants and subjected to Western blot analyzes using CP and phosphoserine antibodies. The presence of corresponding bands at the CP size suggested that CP is phosphorylated *in vivo* (Fig. 1A). Phospho. ELM database and NetPhosK server were used to analyze putative phosphorylation sites of CMV CP (Dinkel et al., 2011; Blom et al., 1999) and the Ser at position 148 was selected as a feasible site of phosphorylation. Amino acid sequence comparison involving several CMV CPs showed that 148 Ser is highly conserved at this position. To investigate whether this aa is phosphorylatable in this position, alanine was introduced to position 148 creating mutant CP/S148A. Next, Rs-CP and CP/S148A mutants were expressed in *E. coli* and subjected to Western blot analyses using phosphoserine and CP antibodies (Fig. 1B). The contrast between the phosphoserine antibody detected Rs-CP and CP/S148A protein bands indicated that position 148 is phosphorylated (Fig. 1B). We performed phosphoprotein staining with the bacterially expressed proteins as well. The difference between Rs-CP and CP/S148A confirmed obviously the phosphorylation of position 148 (Fig. 1B). The bacterially expressed proteins were incubated with Lambda Protein Phosphatase (Lambda PP) or were incubated with its buffer (served as negative control). The samples were detected with phosphoserine and CP antibodies. The difference between the non-treated and treated Rs-CP indicated that Rs-CP is phosphorylated while in the case of CP/148A phosphorylation was not detected (Fig. 1C).

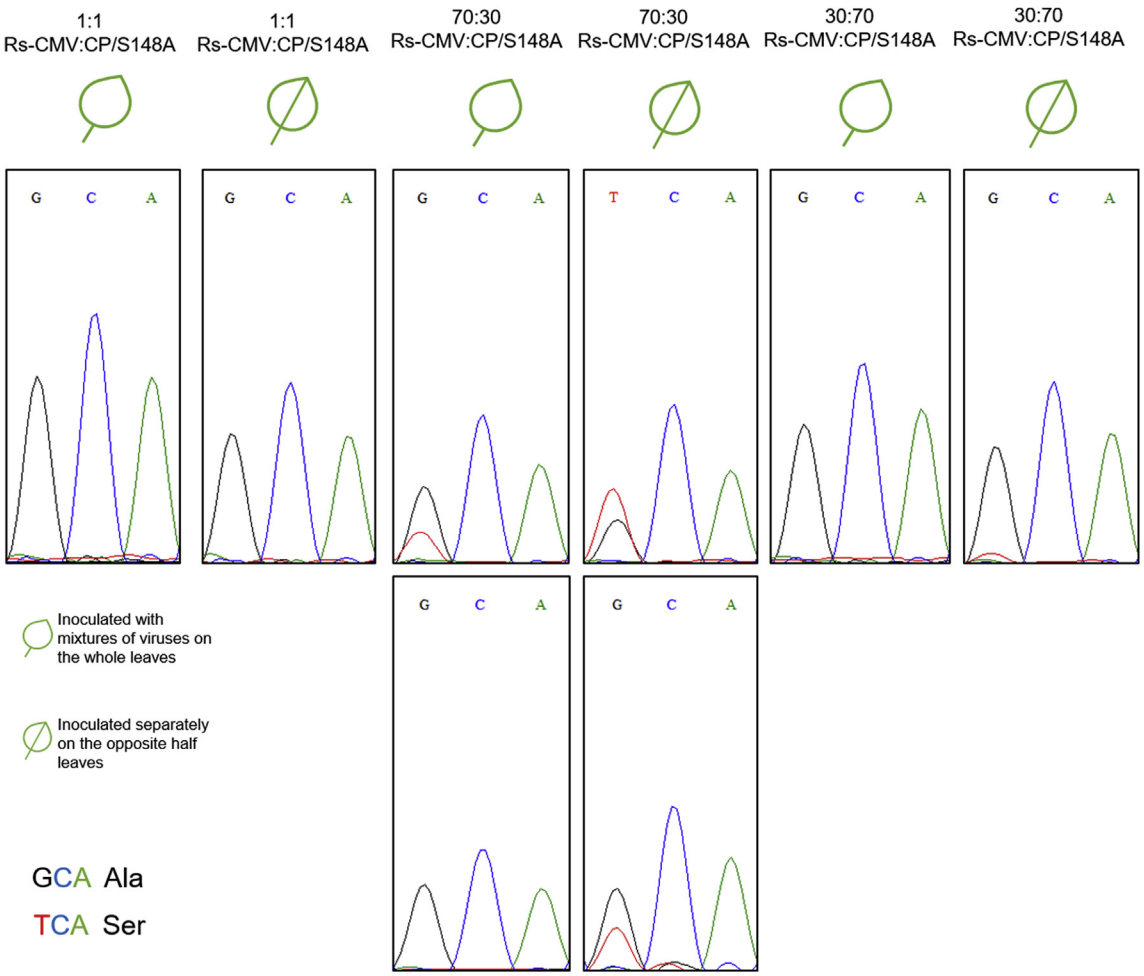

Fig. 4. Sequence analysis of viral progeny in mixed infection with Rs-CMV and CP/S148A mutant. The fitness of the CP/S148A mutant was evaluated in competition experiments. *N. tabacum* L. cv Xanthi plants were inoculated with mixture of virions of Rs-CMV and CP/S148A mutants. Rs-CMV and CP/S148A mutant were inoculated in mixture in the ratio of 1:1 on whole leaves, or separately on the opposite half leaves. Inoculation was also implemented in the same way in the ratio of 70-30% of Rs-CMV and CP/S148A and *vice versa*. Chromatograms show the triplets encoding residue CP 148. Upper chromatograms demonstrate nucleotide sequences two weeks post inoculation, while lower chromatograms show nucleotide sequences four weeks post inoculation.

3.2. The effect of CP/S148 phosphorylation on symptom formation and on viral RNA accumulation on Nicotiana tabacum L. cv Xanthi

To determine the potential role of CMV CP Ser 148 phosphorylation, we introduced mutations to the infectious clone of Rs-CMV RNA3 at aa position 148 creating mutant CP/S148A mimicking the non-phosphorylated state, and CP/S148D to mimick the phosphorylated state of the Ser 148. Symptoms appeared on all the infected *N. tabacum* L. cv Xanthi plants 6–8 days after the inoculation. Two weeks after the inoculation, the identity of the mutants was evaluated in the systematically infected leaves with RT-PCR followed by nucleotide sequence determination. While Rs-CMV and CP/S148A were stable in five independent experiments, the CP/S148D mutant was unstable and it mutated to phosphorylatable amino acids, namely Tyr (four times) or Ser (once).

After that, the symptom induction and virus accumulation of the stable CP/S148A mutant and of the wild-type virus (Rs-CMV) were compared. Rs-CMV induced mosaic, mottled leaf and distortion symptoms in *N. tabacum* L. cv Xanthi plants followed by symptom recovery (asymptomatic leaf stages during infection) (Fig. 2A). Symptomless leaf stages are followed by a new mosaic patterned leaves typical for subgroup I CMV isolates. CP/S148A mutant caused severe mosaic in all leaf stages. We found that substituting CP amino acid S148 to A altered the symptom phenotype as the phenomenon of recovery did not occur, the formation of cyclic symptoms ceased entirely (Figs. 2A and 3A). Two weeks after inoculation in the recovered state of Rs-CMV infected plant, the genomic RNA and CP levels were compared. The accumulation of CP in the systemic leaves was assessed with anti-CP monoclonal antibody and the viral RNA accumulation was detected with northern blot analyses. The virus accumulation was considerably different in the upper non-inoculated leaves at this stage of infection. Both the viral RNA and the CP accumulation proved to be much higher in the CP/S148A infected plants than those of the parental Rs-CMV infection (Fig. 2B).

The accumulation of CP was assessed in 14 vertical leaf positions during one month period using anti-CP monoclonal antibody (Fig. 3B, upper two lanes). The level of CP in distinct leaves were in accordance with the symptoms as two recovery stages were detectable in the case of Rs-CMV during the experiment where the level of CP was drastically reduced. At the same time, infection with CP/S148A caused minor differences in CP level in all leaves during infection (Fig. 3B) in line with symptom formation. In leaves L9 and L10, slightly lower CP levels were detected, although much higher than in the same leaf stages of wild-type virus infected plants. By contrast, the second reduction cycle were completely absent in the case of CP/S148A infection. These results indicated that the substitution of S148A prevents the recovery phenotype of CMV in tobacco plants, coordinated with the stabilization of large amount of CP. Next, determining whether the RNA or the amino

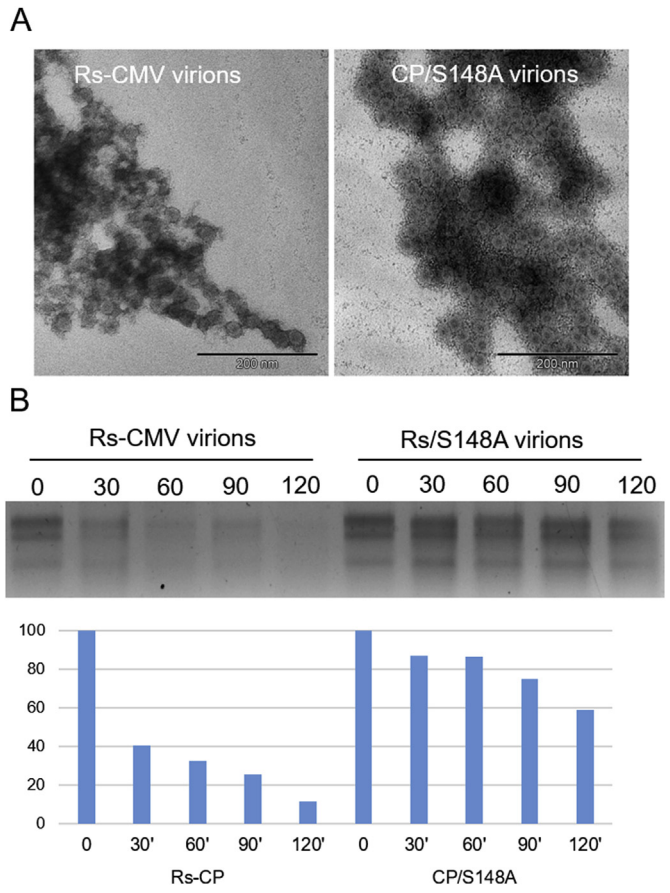

Fig. 5. Virus particle formation and virion stability. (A) TEM of purified virions from systemically infected leaves of *N. tabacum* L. cv Xanthi with Rs-CMV or Rs/S148A mutant. All images are at the same magnification. Scale bars = 200 nm. (B) RNase protection assay of purified Rs-CMV and Rs/S148A mutant virions from *N. tabacum* L. cv Xanthi plants. Virions (10 µg) were incubated with RNase A (0.02 µg/µl) for 0, 30, 60, 90 and 120 min, followed by RNA extraction. Two µl were run in agarose gel and measured using AlphaView software band analysis/densitometry function. The amount of RNAs purified at time zero were taken as 100% and further purified RNAs were compared to time zero.

acid sequence is crucial in symptom formation (since symptom recovery is generally connected to the induction of RNA silencing (Ratcliff et al., 1997)), a silent mutant was created, namely CP/S148sil. In this mutant the coding region of position 148 was mutated but the aa sequence of the Rs-CMV CP was unaffected. The silent mutant caused similar symptoms as the wild-type virus, with cyclic recovered-diseased leaf stages. The Western blot analysis supported the visual observation (Fig. 3A and B, lower panel). The aforementioned CP/S148D mutant was unstable, so we could not involve this mutant in this experiment.

3.3. The effect of S148A mutation on viral fitness

The fitness of the CP/S148A mutant in virus accumulation was evaluated in competition experiments. *N. tabacum* L. cv Xanthi plants were inoculated with the Rs-CMV and the CP/S148A mutant in a mixture and also separately on half leaves. Two weeks post inoculation the ratio of the virus in the systemically infected leaves was evaluated by the nucleotide sequence determination of the RT-PCR product of the CP. The chromatograms demonstrated that the S148A virus has detectable advantage in virus accumulation in systemic leaf over the wild-type virus (Rs-CMV) (Fig. 4). The results were identical if Rs-CMV and CP/148A mutant were inoculated in ratio 1:1 as a mixture on the whole leaf or separately on the opposite half of the leaves. Generally, the competitiveness of CP/S148A mutant is much higher than the wild-type virus. The presence of Rs-CMV was detectable only in plants infected with the ratio 70-30% to Rs-CMV, but the accumulation of the Rs-CMV was only higher in the case where the viruses were infected separately on opposite half leaves (Fig. 4). Four weeks after the inoculation (Fig. 4, lower chromatogram) even in these plants the CP148A was more competitive, since the wild-type Rs-CMV was not detectable in the case of infection in mixture, while in the case of opposite half leaves infection it was still present, but as a minor component.

3.4. Virus particles formation and virion stability

After determining that aa position 148 is involved in formation of cyclic phenomenon of CMV infection, and since stable virion is essential for systemic infection, we analyzed the virion formation and stability of the wild-type and the CP/S148A mutant viruses. Transmission electron microscopy observation of virions purified from infected *N. tabacum* L. cv Xanthi leaves showed no significant difference, Rs/S148A could form similar viral particles as the wild-type virus (Rs-CMV), 25.25 and 25.11 nm, respectively (Fig. 5). This suggested that the formation of the virions was not influenced by the S148A mutation. RNase sensitivity assay was performed by incubating the purified virions for a period of 0–120 min at room temperature in the presence of RNase A followed by viral RNA extraction. Equal amounts (2 µl) were run in agarose gel and measured using AlphaView software band analysis/densitometry function (Fig. 5). Rs-CMV gRNAs were partially degraded after 30 min, and 2 h later the gRNAs were completely degraded. In the case of Rs/S148A mutant the gRNAs were only partially degraded after 120 min (Fig. 5). These results showed that Rs/S148A virion is more stable than the wild-type virion. Alanine substitution at position 148 increases the stability of the virion.

3.5. Effect of CP and mutants on 2b-mediated local GFP-silencing

Previous studies demonstrated that cyclic symptom expression and symptom recovery are associated with RNA silencing (Fukuzawa et al., 2010; Ratcliff et al., 1997) and a recent study demonstrated that CP has negative effects on VSR (viral suppressor of RNA silencing) activities of the 2b protein (Zhang et al., 2017). We examined the effects of wild-type CP (Rs-CMV) and the mutants (CP/S148A and CP/S148D) on the silencing activity of 2b protein in infiltrated patches using Agrobacterium-mediated transient assay. Binary vector expressing GFP reporter gene was agroinfiltrated into transgenic *Nicotiana benthamiana* (silenced for GFP expression) leaves together with the binary vector expressing the wild-type 2b protein co-expressed with vector expressing wild-type CP (Rs-CMV), CP/S148A or CP/S148D, respectively. The suppressor activities were monitored by visual observation of the GFP fluorescence and quantified by measuring the accumulation level of GFP mRNA in the infiltrated leaves by qRT-PCR (Fig. 6A, C).

Coincident with a previous study, we found that co-infiltrating with CP caused reduction in the silencing suppressor activity of the 2b protein so in the presence of CP, 2b protein is less capable to suppress local silencing (Fig. 6). Co-infiltrating with CP/S148A and CP/S148D significantly attenuated the 2b-mediated suppression of GFP silencing as well (Fig. 6). The visual observation in five independent experiments suggested that in the case of CP/S148D mutant the GFP fluorescence is less reduced than in the case of the wild-type CP while CP/S148A resulted in weaker suppression of GFP silencing (Fig. 6A). The presence of the CPs, GFP and 2b protein were verified by Western blot analysis using monoclonal CP, GFP and 2b protein antibodies, respectively (Fig. 6B). GFP mRNA levels in the presence of the suppressor and CPs were determined by qRT-PCR, which confirmed the visual observation (Fig. 6C).

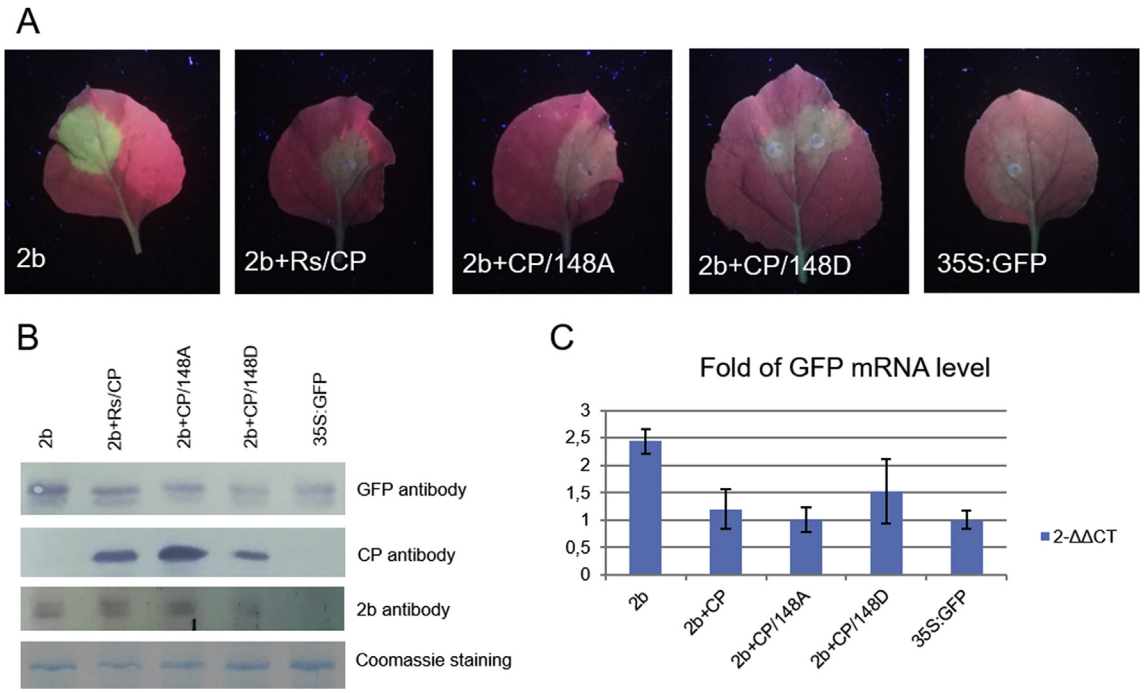

Fig. 6. Effect of CP and mutants on 2b-mediated local GFP-silencing suppression. (A) GFP fluorescence in *N. benthamiana* patches agroinfiltrated with binary vector expressing GFP reporter gene or co-infiltrated with binary vector expressing 2b protein, wild-type CP (Rs-CMV) or mutant CP proteins (CP/S148A and CP/S148D), respectively. (B) Immunoblot analysis of proteins extracted from infiltrated patches. Accumulation of GFP by GFP antibody detection, the accumulation of CP by CP antibody detection and the accumulation of 2b using 2b antibody detection in agroinfiltrated patches. Coomassie staining to monitor the equivalence of protein loading. (C) Accumulation of GFP mRNA in agroinfiltrated patches measured by qRT-PCR.

3.6. Symptoms and virus accumulation in pepper and tomato

To examine the effect of the CP phosphorylation in economically important hosts, *Capsicum annuum* cv. Brendon and *Solanum lycopersicum* cv. Moneymaker plants were inoculated with the wild-type and the CP/S148A mutant viruses. Rs-CMV induced mild mosaic symptoms on pepper and on tomato as well (Fig. 7A and B). CP/S148A mutant caused more severe symptoms with severe stunting on pepper and on tomato as well (Fig. 6A and B). Interestingly, CP accumulation did not increased significantly parallel to the severity of the symptoms (Fig. 7C).

4. Discussion

Symptom recovery is a well-known phenomenon of plant virus infection defined by the emergence of asymptomatic leaves following a systemic symptomatic infection (reviewed by Ghoshal and Sanfacon, 2015). Generally, the virus accumulation is drastically reduced in the recovered leaves, although the virus is present and can cause mild or no symptoms at all in the newly emerging leaves and secondary virus infection is hampered. This phenomenon is generally associated with antiviral RNA silencing (Ratcliff et al., 1997), a sequence specific RNA degradation (Ding and Voinnet, 2007). In the case of different viruses, the role of various silencing mechanisms were proved in recovery, for example sequence specific degradation of viral RNAs (Ding and Voinnet, 2007), where recovered tissue were shown to undergo a posttranscriptional degradation of the viral RNA (Dougherty et al., 1994; Guo and Garcia, 1997), a translational repression (Ma et al., 2015) and a modification of plant gene expression (Lindbo et al., 1993).

CMV induces specific recovery phenotype, namely cyclic mosaic symptoms on *Nicotiana tabacum* L. cv Xanthi plants (Sunpapao et al., 2011). CMV strains generally induce mosaic symptoms on infected tobacco plants followed by recovered, symptomless leaves. The typical symptoms appear on the newly emerging leaves which is followed by a recovery phase after a while, and this cyclic phenomenon can subsist during the entire cultivation of the host. The viral RNA titer changes parallel to the symptomatic phenotype (Ohki et al., 1990). Our results also demonstrated the parallel cyclic feature of the mosaic symptoms and the virus titer in *N. tabacum* L. cv Xanthi plants infected with Rs-CMV (Fig. 3). First time, cycling symptoms of CMV were connected to the MP level in tobacco, since in the case of a specific CMV strain (Sny) with high level of MP showed rather chronic symptoms instead of cycling (Gal-On et al., 1996). According to a recent study, the MP has an effect on the suppression of host pathogen-associated molecular pattern triggered immune responses, and a higher level of MP can have a more reduced immune response resulted in elevated symptomatology (Kong et al., 2018). Several other studies indicated the role of gene silencing in the recovery phenotype in the case of CMV as well. The HC-Pro of potato virus Y (PVY) was proved to cancel successfully the cycling symptoms of CMV (Fukuzawa et al., 2010). The 2b protein of CMV Pepo strain was found to be responsible for transient meristem invasion of the CMV (Sunpapao et al., 2009). In a double mutant tobacco line (dcl24i), the cycling symptom of CMV was also failed (Sunpapao et al., 2014). Lately, the role of CP was proved, since alanine substitution in the N-terminal region of the CP persistently invade the shoot apical meristems of *Nicotiana benthamiana* (Zhang et al., 2017). Our experiments confirmed the role of CP in recovery phenotype. Additionally, we demonstrated that a single aa change is responsible for this trait. Namely, replacing the phosphorylatable Ser with Ala in the aa position 148 abolishes the cyclic phenomenon (Figs. 2 and 3).

Protein phosphorylation is a reversible protein modification, which may have an effect on protein structure, function, protein-protein interactions or protein-RNA interactions and as a reversible modification it can be responsible for switch between different functions (Nishi et al., 2011). This feature can provide an excellent background to coordinate a cycling phenomenon. Interestingly, the modification mimicking the phosphorylated state (CP/S148D) was not stable, but the mutations in the course of infections resulted in phosphorylatable aa in each independent experiment. This suggests that the phosphorylation has a substantial role, such as in correct timing and balancing the host –virus

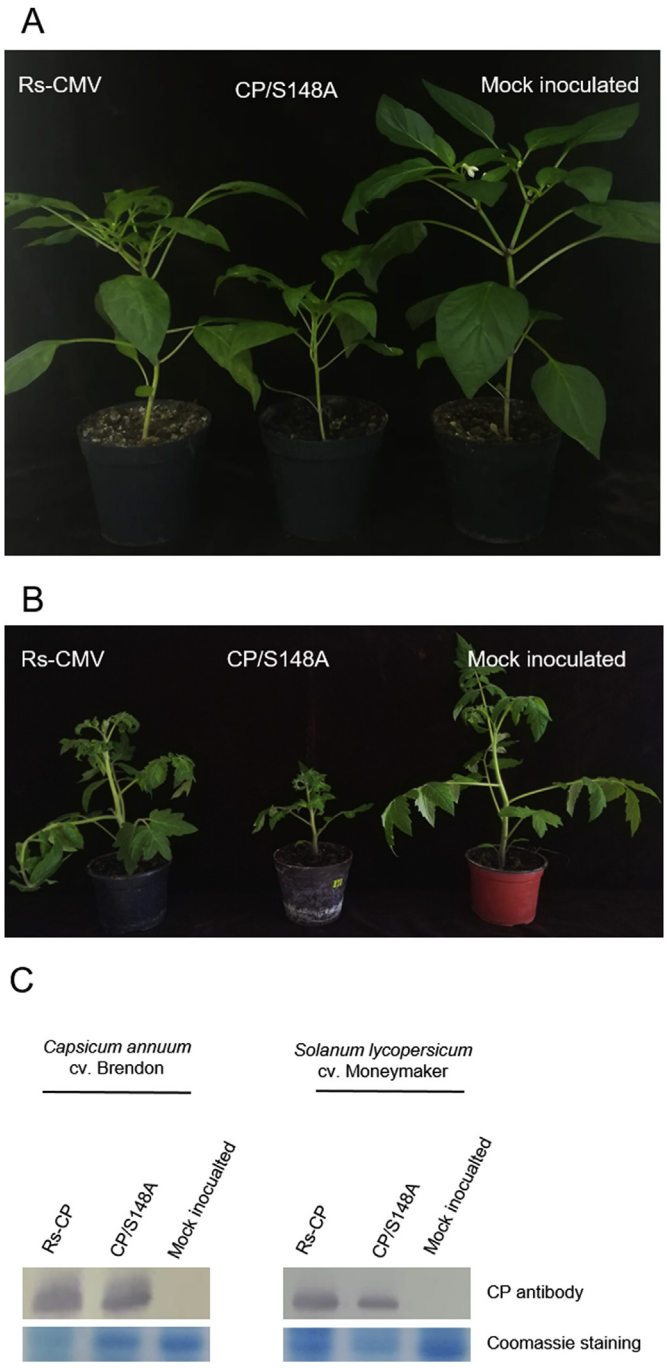

Fig. 7. Symptoms and virus accumulation in pepper and tomato. (A) Symptoms induced by Rs-CMV and CP/S148A mutant on *Capsicum annuum* cv Brendon and on (B) *Solanum lycopersicum* cv Moneymaker plants. (C) CP accumulation in systemically infected leaves using CP antibodies. Coomassie staining shows the equivalent amount of protein loading.

interaction. Mimicking the phosphorylation (at four identified phosphotarget sites) also prevents plum pox virus infection in *Prunus persica* and weakens infection in *Nicotiana benthamiana* and in this case second site mutation occurred (Martínez-Turiño et al., 2018).

Transmission electron microscopy observation of virions purified from infected *N. tabacum* L. cv Xanthi leaves showed no difference in the morphologies of the CPs since CP/S148A could form similar virus particles as the wild-type virus (Rs-CMV) (Fig. 5). The diameter of the virions were nearly identical, but the stability of the virions were significantly different (Fig. 5, lower panel). The CMV virion is composed of 180 CP subunits with T = 3 quasi-icosahedral symmetry. Phosphorylated subunits could also be assembled into the virion in position dependent manner. Serine is an aa with polar hydroxyl side chain, while Ala side chain is the smallest one with hydrophobic property. S148 position is located inside the protein shell of the virion (Fig. 8). The difference in size and charge of the WT and CP/S148A proteins can result in different stability. A negative charge at position 148 (Asp) can cause even more drastic change in the protein-protein interaction between the CP subunits. Eventually, this may promote the instability of the CP/S148D mutant (Fig. 8). According to the electrostatic surface view of the mutant CP/S148D, the phosphorylated CP can be present in monomeric form favoring the facilitation of RNA replication and/or translation, whereas at non-phosphorylated state they may reduce these processes for the sake of virion assembly. The CP phosphorylation of potato virus A (Ivanov et al., 2001), bamboo mosaic virus (Hung et al., 2014) and brome mosaic virus (Hoover et al., 2016) has similar consequence since the affinity to vRNA was reduced and inhibited its binding to vRNA and could enhance the disassembly of the virus (in the primary infected cells). In the case of brome mosaic virus, the phosphatase treatment of the virion reduced its sensitivity to RNase A indicating the enhanced stability of the virion assembled with non-phosphorylated CPs. However, the phosphorylation does not prevent virion assembly generally. In the case of beet black scorch virus, the CP phosphorylation has opposite effect because an alanine mutation which is not phosphorylated at that position decreased the virion stability (Zhao et al., 2015).

Our experiments support the recently demonstrated results as the CMV CP of CMV reduces the 2b-mediated suppression of local gene silencing (Zhang et al., 2017). Moreover, alanine substitution of the N-terminal arginine-rich region of the CP can diminish this effect (Zhang et al., 2017). We found that Rs-CMV CP, mutant CP/S148A and CP/S148D hampers the suppressor activity of 2b protein (Fig. 6) even if the CP/S148D mutant was not stable in infection experiments. Correct timing and balance of phosphorylation are necessary through the regulation of gene silencing suppressor activity and virion assembly, respectively. Many viruses encode weak or transiently active suppressors and presumably they use RNA silencing thereby limiting their accumulation to prevent damaging symptoms on their hosts. These symptom recovery facts have already been revealed in a few studies (Martin-Hernandez and Baulcombe, 2008; Ghoshal and Sanfaçon, 2015).

The experiments carried out on specific test plants like *Nicotiana* species help us to understand the different interactions between viruses and their hosts leading to diseases and viral symptoms. However, these mechanisms can differ greatly in crops (Truniger and Aranda, 2009). Therefore, we were curious about the effect of the CP mutations at position 148 on economically important hosts of CMV. The inoculation of horticultural crops demonstrated that the effect of the CP/S148A mutant virus was also apparent, the symptoms were more severe compared to the parental Rs-CMV strain (Fig. 7). Based on these observations, we propose that the CP phosphorylation has importance in balancing between the intensity of virus infection and the damage on the host. The fine tuning of the phosphorylation state of the CP is a pivotal point and it may have role in protecting host from catastrophic response maintaining the long-term coexistence of the virus and the host.

Here, in this study we provided data about the role of phosphorylation of CMV CP. We provide further evidence that besides the 2b suppressor protein, the CP has also a role in symptom recovery (Zhang et al., 2017), and this is connected to its phosphorylation. The CP/S148A mutation equilibrate the accumulation of the virus during the infection both at RNA and protein level, and it hinders the recovery phenomenon in *N. tabacum* L. cv Xanthi plants (Figs. 2 and 3). Phosphorylation of plant viral proteins reduces RNA-binding due to repulsion of the negative charges between the phosphorylated amino acids and the negatively charged sugar-phosphate backbone of RNAs (Ivanov

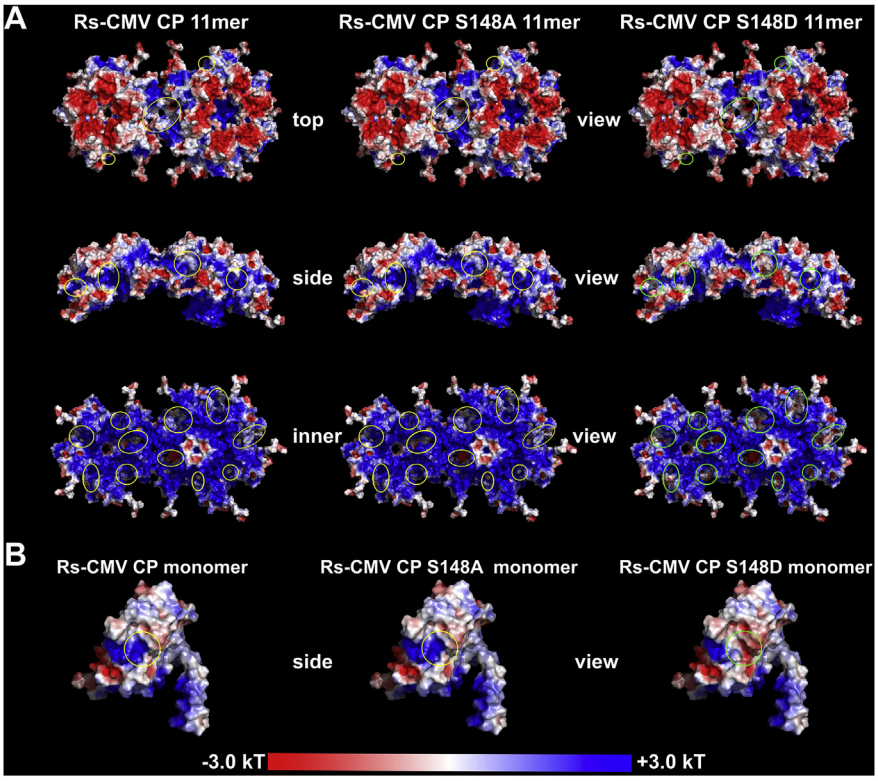

Fig. 8. Electrostatic surface view of the wild and mutant Rs-CMV CP 11-mers (A) and monomers (B). Red represents regions with potential value less than −3.0 kT; white represents 0.0; blue shows regions greater than +3.0 kT. Regions around position 148 are encircled in order to easily recognize the electrostatic changes.

et al., 2001; Nemes et al., 2017). We hypothesize that the S148A mutant has an increased gRNA binding affinity due to the reduction of negative charge (Figs. 5 and 8).

Future studies needed to elicit specific interactions and the regulation of CP by phosphorylation at different stages of the viral life cycle, such as RNA replication, translation and virion assembly.

Conflict of interest

The authors declare that they have no conflict of interest.

Ethical approval

This article does not contain any studies with human participants or animals performed by the authors.

Acknowledgements

Katalin Nemes was the recipient of Bolyai Janos Fellowship of Hungarian Academy of Sciences. The project was supported by OTKA 109482.

References

Atabekov, J.G., Rodionova, N.P., Karpova, O.V., Kozlovsky, S.V., Novikov, V.K., Arkhipenko, M.V., 2001. Translational activation of encapsidated potato virus X RNA by coat protein phosphorylation. Virology 286 (2), 466–474.
Baker, N.A., Sept, D., Joseph, S., Holst, M.J., McCammon, J.A., 2001. Electrostatics of nanosystems: application to microtubules and the ribosome. Proc. Natl. Acad. Sci. 98, 10037–10041.
Blom, N., Gammeltoft, S., Brunak, S., 1999. Sequence- and structure-based prediction of eukaryotic protein phosphorylation sites. J. Mol. Biol. 294 (5), 1351–1362.
Chapdelaine, Y., Kirk, D., Karsies, A., Hohn, T., Leclerc, D., 2002. Mutation of capsid protein phosphorylation sites abolishes Cauliflower mosaic virus infectivity. J. Virol. 76, 11748–11752.
Chen, B., Francki, R.I.B., 1990. Cucumovirus transmission by the aphid Myzus persicae is determined solely by the viral coat protein. J. Gen. Virol. 71, 939–944.
Ding, S.W., Voinnet, O., 2007. Antiviral immunity directed by small RNAs. Cell 130, 413–426.
Dinkel, H., Chica, C., Via, A., Gould, C.M., Jensen, L.J., Gibson, T.J., Diella, F., 2011. Phospho.ELM: a database of phosphorylation sites - update 2011. Nucleic Acids Res. 39 (Suppl. l_1), D261–D267.
Diveki, Z., Salanki, K., Balazs, E., 2004. The Necrotic Pathotype of the Cucumber mosaic virus (CMV) Ns strain is solely determined by amino acid 461 of the 1a protein. Mol. Plant Microbe Interact. 17, 837–845.
Dolinsky, T.J., Nielsen, J.E., McCammon, J.A., Baker, N.A., 2004. PDB2PQR: an automated pipeline for the setup, execution, and analysis of Poisson-Boltzmann electrostatics calculations. Nucleic Acids Res. 32, 665–667.
Dougherty, W.G., Lindbo, J.A., Smith, H.A., Parks, T.D., Swaney, S., Proebsting, W.M., 1994. RNA-mediated virus resistance in transgenic plants: exploitation of a cellular pathway possibly involved in RNA degradation. Mol. Plant Microbe Interact. 7 (5), 544–552.
Edwardson, J.R., Christie, R.G., 1991. Cucumoviruses. 293-319. CRC Handbook of Viruses Infecting Legumes. CRC Press, Boca Raton, Fla.
Fukuzawa, N., Itchoda, N., Ishihara, T., Goto, K., Masuta, C., Matsumura, T., 2010. HC-Pro, a potyvirus RNA silencing suppressor, cancels cycling of Cucumber mosaic virus in Nicotiana benthamiana plants. Virus Genes 40 (3), 440–446.
Gal-On, A., Kaplan, I.B., Palukaitis, P., 1996. Characterization of Cucumber mosaic virus: II. Identification of movement protein sequences that influence its accumulation and systemic infection in tobacco. Virology 226, 354–361.
Ghoshal, B., Sanfaçon, H., 2015. Symptom recovery in virus-infected plants: revisiting the role of RNA silencing mechanisms. Virology 479–480, 167–179. https://doi.org/10.1016/j.virol.2015.01.008.
Gilson, M.K., Sharp, K.A., Honig, B., 1987. Calculating electrostatic interactions in biomolecules: method and error assessment. J. Comput. Chem. 9, 327–335.
Guo, H.S., Garcia, J.A., 1997. Delayed resistance to plum pox potyvirus mediated by a mutated RNA replicase gene: involvement of a gene silencing mechanism. Mol. Plant Microbe Interact. 10, 160–170.
Hoover, H.S., Wang, J.C., Middleton, S., Ni, P., Zlotnick, A., Vaughan, R.C., Kao, C.C., 2016. Phosphorylation of the brome mosaic virus capsid regulates the timing of viral infection. J. Virol. 90 (17), 7748–7760.
Humphrey, W., Dalke, A., Schulten, K., 1996. VMD - visual MolecularDynamics. J. Mol. Graph. 14, 33–38.
Hung, C.J., Huang, Y.W., Liou, M.R., Lee, Y.C., Lin, N.S., Meng, M., Tsai, C.H., Hu, C.C., Hsu, Y.H., 2014. Phosphorylation of coat protein by protein kinase CK2 regulates cell-to-cell movement of Bamboo mosaic virus through modulating RNA binding. Mol. Plant Microbe Interact. 27 (11), 1211–1225. https://doi.org/10.1094/MPMI-04-14-0112-R.
Ivanov, K.I., Puustinen, P., Merits, A., Saarma, M., Mäkinen, K., 2001. Phosphorylation down-regulates the RNA binding function of the coat protein of potato virus A. J. Biol. Chem. 276, 13530–13540.
Ivanov, K.I., Puustinen, P., Gabrenaite, R., Vihinen, H., Rönnstrand, L., Valmu, L., Kalkkinen, N., Mäkinen, K., 2003. Phosphorylation of the potyvirus capsid protein by protein kinase CK2 and its relevance for virus infection. Plant Cell 15 (9), 2124–2139. https://doi.org/10.1105/tpc.012567.
Johansen, L.K., Carrington, J.C., 2001. Silencing on the spot. Induction and suppression of

RNA silencing in the agrobacterium-mediated transient expression System 1. Plant Physiol. (Wash. D C) 126 (3), 930–938.
Kaplan, I.B., Gal-On, A., Palukaitis, P., 1997. Characterization of cucumber mosaic virus. III. Localization of sequences in the movement protein controlling systemic infection in cucurbits. Virology 230 (2), 343–349.
Kim, S.H., Palukaitis, P., Park, Y.I., 2002. Phosphorylation of cucumber mosaic virus RNA polymerase 2a protein inhibits formation of replicase complex. EMBO J. 21 (9), 2292–2300.
Kong, J., Wei, M., Li, G., Lei, R., Qiu, Y., Wang, C., Li, Z., Zhu, S., 2018. The cucumber mosaic virus movement protein suppresses PAMP-triggered immune responses in Arabidopsis and tobacco. Biochem. Biophys. Res. Commun. 498 (3), 395–401.
Lindbo, J.A., Silva-Rosales, L., Proebsting, W.M., Dougherty, W.G., 1993. Lnduction of a highly specific antiviral state in transgenic plants: lmplications for regulation of gene expression and virus resistance. The Plant Cell 5, 1749–1759.
Lõhmus, A., Hafrén, A., Mäkinen, K., 2017. Coat protein regulation by CK2, CPIP, HSP70, and CHIP is required for potato virus a replication and coat protein accumulation. J. Virol. 91 (3) e01316-16.
Lot, H., Marrou, J., QuIor, J.B., Esvan, C.H., 1972. Contribution á l'étude de virus de la mosaique du concombre (CMV). — II. Methode de purification rapide du virus. Ant. Phytopath. 4, 25–38.
Lucy, A.P., Guo, H.S., Li, W.X., Ding, S.W., 2000. Suppression of post-transcriptional gene silencing by a plant viral protein localized in the nucleus. EMBO J. 19, 1672–1680.
Ma, X., Nicole, M.C., Meteignier, L.V., Hong, N., Wang, G., Moffett, P., 2015. Different roles for RNA silencing and RNA processing components in virus recovery and virus-induced gene silencing in plants. J. Exp. Bot. 66, 919–932.
Martin-Hernandez, A.M., Baulcombe, D.C., 2008. Tobacco rattle virus 16-kilodalton protein encodes a suppressor of RNA silencing that allows transient viral entry in meristems. J. Virol. 82, 4064–4071.
Martínez-Turiño, S., Pérez, J.J., Hervás, M., Navajas, R., Ciordia, S., Udeshi, N.D., Shabanowitz, J., Hunt, D.F., García, J.A., 2018. Phosphorylation coexists with O-GlcNAcylation in a plant virus protein and influences viral infection. Mol. Plant Pathol. 19 (6), 1427–1443.
Matsushita, Y., Yoshioka, K., Shigyo, T., Takahashi, H., Nyunoy, H., 2002. Phosphorylation of the movement protein of cucumber mosaic virus in transgenic tobacco plants. Virus Genes 24 (3), 231–234.
Nemes, K., Gellért, Á., Balázs, E., Salánki, K., 2014. Alanine scanning of cucumber mosaic virus (CMV) 2B protein identifies different positions for cell-to-cell movement and gene silencing suppressor activity. PLoS One 9 (11), e112095.
Nemes, K., Gellért, Á., Almási, A., Vági, P., Sáray, R., Kádár, K., Salánki, K., 2017. Phosphorylation regulates the subcellular localization of Cucumber Mosaic Virus 2b protein. Sci. Rep. 7, 13444.
Nishi, H., Hashimoto, K., Panchenko, A.R., 2011. Phosphorylation in protein-protein binding: effect on stability and function. Structure 19 (12), 1807–1815.
Ohki, S.T., Takami, Y., Inouye, T., 1990. Accumulation of double-stranded RNAs 3 and 4 in the symptomless leaves and green areas of mosaic-affected leaves of tobacco plants infected with cucumber mosaic virus. Ann. Phytopathol. Soc. Jpn. 56, 213–218.
Palukaitis, P., García-Arenal, F., 2003. Cucumoviruses. Adv. Virus Res. 62, 241–323.
Qiu, Y., Zhang, Y., Wang, C., Lei, R., Wu, Y., Li, X., Zhu, S., 2018. Cucumber mosaic virus coat protein induces the development of chlorotic symptoms through interacting with the chloroplast ferredoxin I protein. Sci. Rep. 8 (1), 1205. https://doi.org/10.1038/s41598-018-19525-5.
Ratcliff, F., Harrison, B.D., Baulcombe, D.C., 1997. A similarity between viral defense and gene silencing in plants. Science 276 (5318), 1558–1560.
Ryu, K.H., Kim, C.H., Palukaitis, P., 1998. The coat protein of cucumber mosaic virus is a host range determinant for infection of maize. Mol. Plant Microbe Interact. 11 (5), 351–357.
Sambrook, J., Fritsch, E.F., Maniatis, T., 1989. Molecular Cloning: a Laboratory Manual, second ed. Cold Spring Harbor Laboratory Press.
Scholthof, K.B., Adkins, S., Czosnek, H., Palukaitis, P., Jacquot, E., Hohn, T., Hohn, B., Saunders, K., Candresse, T., Ahlquist, P., Hemenway, C., Foster, G.D., 2011. Top 10 plant viruses in molecular plant pathology. Mol. Plant Pathol. 12 (9), 938–954.
Schrödinger, L., 2019. Schrödinger Suite. Schrödinger, LLC, New York, NY.
Smith, T.J., Chase, E., Schmidt, T., Perry, K.L., 2000. The structure of cucumber mosaic virus and comparison to cowpea chlorotic mottle virus. J. Virol. 74, 7578–7586.
Sunpapao, A., Nakai, T., Dong, F., Mochizuki, T., Ohki, S.T., 2009. The 2b protein of cucumber mosaic virus is essential for viral infection of the shoot apical meristem and for efficient invasion of leaf primordia in infected tobacco plants. J. Gen. Virol. 90 (12), 3015–3021.
Sunpapao, A., Mochizuki, T., Ohki, S.T., 2011. Relationship between viral distribution in the leaf primordia/young developing leaves and symptom severity in the fully expanded leaves of tobacco plants infected with Cucumber mosaic virus. Australas. Plant Pathol. 40 (3), 215–221. https://doi.org/10.1007/s13313-010-0027-5.
Sunpapao, A., Mochizuki, T., Ohki, S.T., 2014. Effect of dicer-like proteins 2 and 4 and RNA-dependent RNA polymerase 1 as RNA silencing components on cyclic mosaic symptom development in tobacco infected with the Cucumber mosaic virus. Songklanakarin J. Sci. Technol. 36 (1), 21–26.
Suzuki, M., Kuwata, S., Masuta, C., Takanami, Y., 1995. Point mutations in the coat protein of Cucumber mosaic virus affect symptom expression and virion accumulation in tobacco. J. Gen. Virol. 76, 1791–1799.
Truniger, V., Aranda, M.A., 2009. Recessive resistance to plant viruses. Adv. Virus Res. 75, 119–159.
Wong, S.M., Thio, S.S.C., Shintaku, M.H., Palukaitis, P., 1999. The rate of cell-to-cell movement in squash of cucumber mosaic virus is affected by sequences of the capsid protein. Mol. Plant Microbe Interact. 12 (7), 628–632.
Zhang, X.P., Liu, D.S., Yan, T., Fang, X.D., Dong, K., Xu, J., Wang, Y., Yu, J.L., Wang, X.B., 2017. Cucumber mosaic virus coat protein modulates the accumulation of 2b protein and antiviral silencing that causes symptom recovery in planta. PLoS Pathog. 13 (7), e1006522. https://doi.org/10.1371/journal.ppat.1006522.
Zhao, X., Wang, X., Dong, K., Zhang, Y., Hu, Y., Zhang, X., Chen, Y., Wang, X., Han, C., Yu, J., Li, D., 2015. Phosphorylation of Beet black scorch virus coat protein by PKA is required for assembly and stability of virus particles. Sci. Rep. 5, 11585. https://doi.org/10.1038/srep11585.